IMPROVING THE PERFORMANCE OF BOLTED JOINTS IN COMPOSITE STRUCTURES USING METAL INSERTS

V. Mara[1], R. Haghani[2] and M. Al-Emrani[3]

ABSTRACT

Bolted joints are a common method for joining FRP structures. The main advantage of bolted joints is their detachability, but they bring along shortcomings, such as low joint efficiency, which is even more pronounced in the presence of clearances, and inability to rely on the beneficial effects of bolt preloads due to the considerable losses of bolt preload caused by the creep deformation in the FRP. To tackle these problems, a solution utilising metallic inserts in the hole is proposed in this paper. A series of experimental tests have been conducted to investigate the effect of inserts on the bolt preload relaxation, the stiffness and the load-bearing behaviour of joints. Finite element analyses were also employed. The study demonstrates several benefits of the inserts: the bolt preload relaxation is minimised, the load transfer by friction can be utilised and the joint efficiency is increased in terms of stiffness and strength.

Keywords: B. Stress relaxation; C. Numerical analysis; D. Mechanical testing; E. Joints/joining

1. Introduction

Fibre reinforced polymer (FRP) composite materials are gaining widespread application in bridge construction. The light weight and opportunity to prefabricate FRP elements offer the advantages of modular construction and swift on-site assembly. The on-site assembly of FRP bridge members is commonly performed using mechanical fasteners, mainly bolted. Bolted joints are easy to use on site and offer the potential for disassembly and ease of visual inspection. Investigations into the use of bolted joints for composite structures began in the mid-1960s in the aerospace industry [1]. Research on bolted joints in civil engineering applications started in the early 1990s, focusing primarily on pultruded glass fibre reinforced polymer (GFRP) profiles [2, 3]. One of the major goals of the research into bolted joints has been to determine the effect of various parameters on the mechanical performance of the joints, including: (a) material parameters, such as fibre type, ply orientations and stacking sequence [4-6], (b) fastener parameters, such as fastener type [7, 8], bolt preload [7-9], clearances between bolt and hole [10, 11] and friction between members [12-14], and (c) design parameters, such as joint type and geometric factors [15-17].

Bolted joints can ultimately fail in a number of failure modes, the most common being net-tension, shear-out, bearing or cleavage failure, see Fig.1. Bearing failure is a

[1] PhD student, Dept. of Civil and Environmental Engineering, Division of Structural Engineering, Chalmers University of Technology, Sven Hultins gata 8, SE-412 96 Göteborg, Sweden
Phone. +46 31 772 20 19, E-mail: valbona.mara@chalmers.se
[2] Assistant Professor, Dept. of Civil and Environmental Engineering, Division of Structural Engineering, Chalmers University of Technology, Sven Hultins gata 8, SE-412 96 Göteborg, Sweden
[3] Associate Professor, Dept. of Civil and Environmental Engineering, Division of Structural Engineering, Chalmers University of Technology, Sven Hultins gata 8, SE-412 96 Göteborg, Sweden

preferred failure mode for composite joints due to its progressive and non-catastrophic mode. Owing to its importance, emphasis is placed on bearing failure in the existing research, as well as in this study.

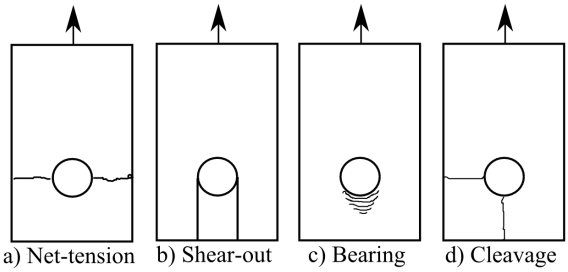

Fig.1. Common failure modes for composite plate-to-plate, single-bolted joints

A study of the literature shows that the research work on FRP mechanical joints focuses on the strength of joints, presented in terms of joint capacity as a function of joint geometry or bolt torque. Less attention is paid to the stiffness of mechanical joints. Stiffness is a crucial requirement in the design of bridges and it is even more important for GFRP bridges due to their stiffness-driven design [18]. One of the main parameters affecting the stiffness of bolted joints is the presence of clearances, which are inevitable to facilitate on-site assembly. Clearances reduce the stiffness and the damage initiation load of joints and can induce slip between the connected members which needs to be controlled during the service life of the bridge. Slip due to clearances can also cause a reduction in the fatigue life of composite bolted joints, as demonstrated in [11, 19]. Slip can be delayed by the application of preload in the bolts and by taking advantage of friction to transfer loads between connected elements. However, the viscoelastic behaviour of FRP composites makes them susceptible to creep, as a result of which the bolt preload could be relaxed over time. The creep phenomenon in FRPs is more pronounced at high temperature and in moist environments [20]. For this reason, any load transfer by friction is ignored in the design of composite bolted joints and the load transfer mechanism relies solely on bearing in the FRP material. One solution to minimise the slip in FRP bolted joints, which has been proposed by Qureshi and Mottram [21], is to inject resin into the clearance between the hole and the bolt and research on this solution is on-going.

The efficiency of bolted joints, defined as a percentage of the ratio of the joint strength to the strength of the weakest joined member, is low, due to high stress concentrations created by the presence of the hole in the laminate while loading. Hart-Smith [19] demonstrated that the maximum attainable efficiency of bolted composite joints is 40% of the strength of the base material. This limit is not usually relevant for GFRP bridges, due to their stiffness-driven design. The stresses in the serviceability limit state are low and they are additionally limited to 20% of the material strength for creep rupture reasons [22]. This design has its benefits when it comes to robustness, lack of ductility of the material and low joint efficiency. On the other hand, it pinpoints the importance of joint stiffness in the service life of the bridge.

In order to increase joint efficiency, several researchers have proposed the use of metallic inserts, either bonded or interference fit, in the hole between the bolt and the composite laminate. Metallic inserts help to reduce the stress concentrations around the hole in the composite, as observed numerically [23-26] and experimentally [27, 28]. They help to distribute the stresses and strains around the entire hole as long as the

adhesive bond does not fail. The joint efficiency of bolted joints with inserts is increased compared with only-bolted joints and the increase in strength is reported to vary from 10% to 100% in the literature [23, 26, 28, 29]. Inserts with laps have been more efficient than straight circular inserts (see Fig. 2).

Fig. 2. Different types of inserts

The research performed on bolted joints with inserts is focused primarily on the ultimate strength of the joints where the bolts are pretensioned as "finger-tight". To the authors' knowledge, no research has been conducted on the performance of bolted joints with inserts with preloaded bolts. In addition, there is a lack of knowledge of the effect of clearances between the bolt and insert on the performance of the joint.

In this regard, it was of interest to study bolted joints with inserts with bolt preload and clearances. One of the main objectives was to obtain bolted joints in which load transfer by friction is utilised and any slip in the joint in the serviceability limit state (SLS) is prevented. Steel inserts were designed for the purpose of the study, performing the functions of: (i) minimising the relaxation of bolt preload and (ii) resisting the service loads without slip via friction between the insert faces.

A series of experimental tests was conducted to examine the behaviour of these joints. The experimental programme included several types of test to characterise the relevant material properties and to examine different aspects of the joints which were related to the main aim of testing. In addition, numerical analyses were carried out to aid in the understanding and interpretation of various phenomena in the experimental results.

2. Experimental procedure and numerical models

2.1 Material characterisation

The composite material used in the tests consisted of stitched combo mats, which had E-glass rovings in the directions of 0/90 deg or +/–45 deg and polyester as a matrix. The fabric lay-up of the composite laminate was [0/90, +/–45, 0/90, +/–45, $\overline{0/90}$]$_S$, giving a material with the same longitudinal and transverse in-plane properties. The laminates had a fibre volume fraction of approximately 50% and were manufactured using the resin infusion process. The thickness of the laminates varied between 7.0 and 7.5 mm. The material properties were determined by conducting tests on coupon samples in tension, compression and in-plane shear according to ASTM standards [30-32]. The average results of these tests (± standard deviation) are summarised in Table 1. Two elasticity moduli (referred to as E_1 and E_2, in which E_1 corresponds to the first linear region of strain range 0-0.2% and E_2 corresponds to the second linear region of strain range 0.8%-1.5%) have been determined for the tensile tests due to the non-linear stress-strain behaviour of the material, see Fig. 3. The tensile stiffness is substantially reduced at a strain of approximately 0.25%, which is the strain limit of irreversible damage for this material and is attributed to the micro-cracking of the resin. It has also been reported in the existing literature that matrix cracking, which occurs at an early

loading stage in the off-axis plies of the composite material, is the main source of stiffness changes while loading composite laminates [33, 34].

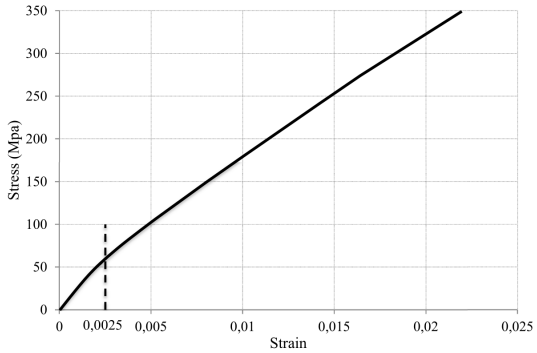

Fig. 3. Typical tensile stress-strain behaviour of the composite material

The Poisson ratio was measured for only two coupons for the tensile tests and the average value was measured as 0.225. For in-plane shear tests, only two specimens could be loaded to failure and the average ultimate strength and strain are given in Table 1.

Table 1. Average properties of the GFRP laminates

Test type	No. of tests	Ultimate strength [MPa]	Ultimate strain (%)	Elasticity modulus [GPa]		Shear modulus [GPa]
				E_1	E_2	
Tensile	6	350 ± 8.4	2.24 ± 0.20	25.83 ± 2.19	14.92 ± 0.61	-
Compressive	5	241.4 ± 8.7	1.02 ± 0.05	25.65 ± 0.45		-
In-plane shear	5	185.2	3.42	-		8.2 ± 0.42

2.2 Joint geometry and test set-up

The type of joint chosen for testing was a double-lap, single-bolted joint to be loaded in shear. The double-lap configuration was selected in order to subject the joint to a concentrically applied load and minimise the secondary bending effects. The joint was designed to promote bearing failure by following the guidelines and recommendations given in the D5961 ASTM test standard [35] and the EuroComp Design Code [22]. The geometry is expressed in terms of ratios between four variables, width (w), bolt hole diameter (d), edge distance (e) and laminate thickness (t) such as: (i) $w/d \geq 6$, (ii) $e/d \geq 3$ and (iii) $d/t = 1.5\text{-}3$. The selected geometry of the joint laminates and the test set-up are illustrated in Fig. 4. It should be noted that the specimen dimensions were also dictated by the laboratory testing machine.

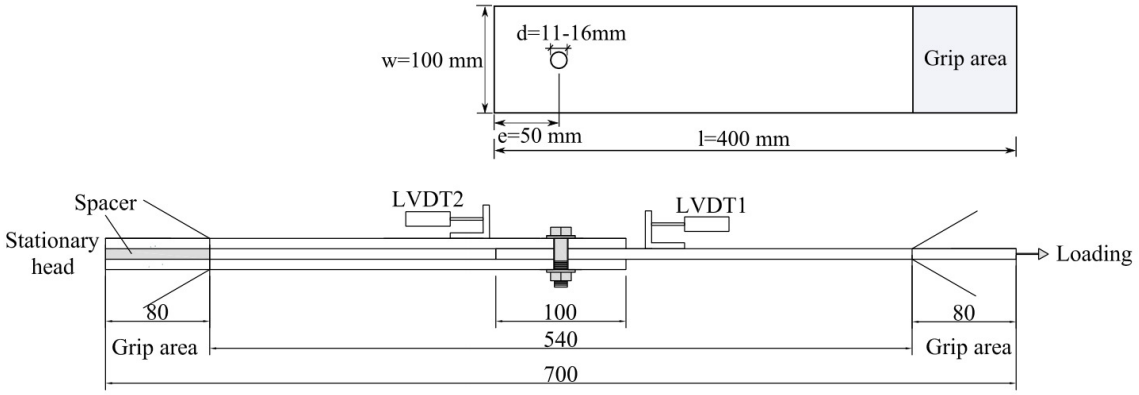

Fig. 4. Illustration of the joint geometry and test set-up

Linear variable differential transducers (LVDT) were used to measure the displacement of the joints. It was observed that the difference between the measured LVDT1 displacements and the relative displacements, LVDT1-LVDT2, was negligible due to the relatively small elongation of the specimen between the grip on the left and the LVDT. The displacement measured from LVDT1 was therefore taken into consideration in the load-displacement curves shown in the following sections. The load was applied in a displacement-controlled manner at a rate of 0.25 mm/min.

Standard steel bolts M10, class 8.8 (i.e. yield strength of 640 MPa and ultimate strength of 800 MPa) were used in all joints. A clearance of 1 mm was chosen for the joint tests based on the common range of clearances used in steel bridges for bolt diameters lower than 14 mm. As a result, a hole of 11 mm was drilled in the only-bolted joints, whereas, in the joints with inserts, the hole was 16 mm in diameter in order to fit the insert (see insert geometry in Section 2.3). In joints without inserts, washers with an outer diameter of 22 mm and a thickness of 1.9 mm were used.

An overview of the different types of investigated joint, together with their respective designations and objectives in the study, is given in Table 2. Additional necessary specifications and the results of all the tests are given in Section 3.

Table 2. Overview of the experimental tests

Set	Test type	Designa-tion	No. of tests	Bolt preload (kN)	Objective
1	Only-bolted joint	B	3	Finger tightened	Reference test
2	Bolted joint with insert	BI	3	Finger tightened	To check the effect of inserts and for the sake of comparison with the specimens with insert and bolt preload
3	Bolted joint with pre-tensioned bolts	BP	5	~25kN	To examine the change in strength and stiffness when bolt preload is applied and to compare with the other joint types
4	Bolted joint with insert and bolt preload	BIP, BIPF*	10	~25 kN	To examine the behaviour of the joints with inserts when bolt preload is applied
5	Relaxation tests of bolted joints without and with insert	RBP, RBIP	6	~25 kN	To examine the relaxation of the bolt preloads of the joints with and without inserts

*BIPF specimens have insert surfaces with higher coefficients of friction

2.3 Metallic insert geometry and bolt preload selection

The geometry of the inserts designed for the purpose of this study is shown in Fig. 5. Steel material class S355 was used. Inserts with laps were selected for use in this study. As mentioned in the introduction, existing research shows that inserts with laps are the most effective geometry for increasing the efficiency of joints. In addition, the laps are necessary, because it is the friction between the insert surfaces which is utilised to transfer forces when bolt preload is provided. The geometry and dimensions of the metallic inserts were based on preliminary numerical analyses and the potential for production. The assembly of the inserts was made possible by threads, as shown in Fig. 5. The inserts were designed to bear a load of at least 30 kN in compression without yielding. Preliminary testing of the inserts showed that the insert was able to support a load of up to 40 kN before yielding.

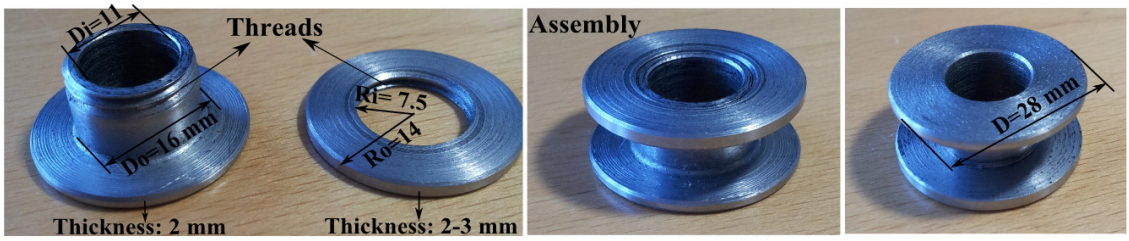

Fig. 5. Configuration of the steel inserts and their dimensions in mm

Regarding the bolt preload, it was a question of how much bolt preload could be applied to the composite joints. One factor that limits the maximum applicable bolt load is the damage to the composite material due to the induced clamping pressure from the bolt preload, which is directly related to the through-thickness compressive strength of the composite material. In aerospace/aircraft applications, the bolt preload values of the threaded fastener joint are limited to 30% of the fastener yield strength for typical preloaded composite structural assemblies in tension [36]. However, Thomas and Zhao [37] demonstrated that this is a very conservative approach and bolt preloads equivalent to the ones used in steel structures can be used. In the EuroComp Design Code and Handbook [22], it is recommended that the clamping pressure on GFRP laminates should not exceed 68 MPa or 1/3 of the through-thickness compressive strength.

In the experiments in this study, it was decided to use bolt preloads in the same range as that recommended in the EuroCode EN1993-1-8 for steel joints [38], which is 70% of the ultimate strength of the bolt. Using standard steel bolts M10, class 8.8, the maximum permissible clamping force is around 32 kN. Due to tightening difficulties, it was decided that the final bolt preload should be 25 kN in all the tests with bolt preload. The clamping pressure to the FRP material was calculated as 86 MPa using equation (1) in a joint without an insert for a bolt preload of 25 kN. No damage was observed in the clamping area for the maximum clamping pressure of 86 MPa. There was only a slight impression of the washer in the laminate due to the thickness waviness in the material.

$$\sigma_{press} = \frac{F_{bolt}}{\frac{\pi}{4} * (D_w^{\,2} - D_i^{\,2})} \qquad (1)$$

where F_{bolt} is the bolt preload, D_w is the outer diameter and D_i is the inner diameter of the washer.

In the event of joints with inserts, the bolt preload is mostly accommodated by the insert and any possible clamping pressure to the laminate is negligible. The bolt preload was controlled by strain gauges installed in the bolts. A hole with a 2 mm diameter was drilled in the centre of the bolt head down into the shank to a depth of 23 mm, where a strain gauge was installed in the hole, which was then filled with adhesive. Once the strain gauges had been installed, the bolts were calibrated to measure the tensile force via the strain gauges within the elastic range of the bolt.

2.4 Numerical modelling

All experimentally investigated joints were numerically modelled using the FEA package, ABAQUS v6.13-3. The modelling technique was kept simple by using only linear-elastic material properties for the composite material, excluding any material degradation schedules. For this reason, the FE analysis was only used to identify failure zones and to understand the load transfer mechanisms and not to predict the ultimate joint failure load. The joints are modelled in three-dimensional order with solid elements, in order to accurately capture the stress components in the model. Thanks to the symmetry, only half the joint was modelled.

The bolt was modelled as an elastic-perfect plastic material with a yield strength of 640 MPa. The nut and fastener shank were merged and assembled as one part in order to reduce the contact surfaces and ensure the shortening of the running time. The threads in the bolt and the inserts were ignored in the FEA models. The steel material for the inserts was also modelled as an elastic-perfect plastic material with a yield strength of 355 MPa. The FRP laminates were modelled as a linear-elastic, orthotropic material based on the data from the material characterisation tests and the literature. The second tensile elasticity modulus was considered and approximated to 15,000 MPa. The material properties are those listed in Table 3.

Table 3. Material properties used for the FE model

Material	Elasticity modulus (MPa)			Poisson's ratio			Shear modulus (MPa)		
	E_x	E_y	E_z	ν_{xy}	ν_{xz}	ν_{yz}	G_{xy}	G_{xz}	G_{yz}
FRP*	15,000	15,000	4,000	0.225	0.40	0.40	8,200	3,000	3,000
Steel	210,000			0.3					

* x, y and z coordinates represent longitudinal, transverse and through-thickness properties, see Fig. 6.

The laminates were modelled with the same dimensions as in the test but without the grip areas. One end of the model was held fixed in the translational directions (U_x, U_y and U_z). The other end had an equation constraint with a reference point (RP), which makes it possible to constrain the motion of regions of the assembly to the motion of the reference point. In this way, the motion of the right end surface, which was held fixed in two translational directions (U_y and U_z), was governed by the motion of the reference node, where *x*-displacements, representing the moving jaw of the test machine in a displacement-control mode, were applied, see Fig. 6.

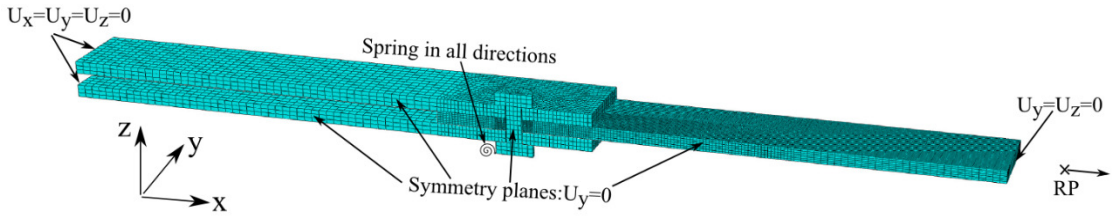

Fig. 6. Boundary conditions of the finite element model

In the models with bolt preload, the load was introduced in two steps. Firstly, the bolt preload was defined using the bolt-load option in ABAQUS. This preload was simulated in Abaqus/Standard by defining a "cutting surface" in the bolt shaft and subjecting it to a normal load along the bolt axis. Once the bolt was pretensioned, the applied bolt load was modified to a "fixed" boundary condition by selecting the "fix at current length" option in step 2. This specifies that the change in the length of the bolt at the "cut surface" remains fixed, while the remainder of the bolt is free to deform in response to the loads on the assembly. In step 2, the displacement-controlled load was also introduced on the specimen.

The contacts between the bolt, insert and FRP laminates were surface-based, with hard contact as normal behaviour and with the classical Coulomb friction model with penalty friction simulation as the tangential behaviour. Surface-to-surface discretisation was employed for the contacts and the finite sliding approach was adopted to track the contact condition. The friction coefficients were set at 0.3 for the laminate-to-laminate surfaces, as measured in the tests described in the next section. Between the insert faces, the coefficient of friction varied between 0.1 and 0.7. The friction coefficient for the remaining contact pairs, such as bolt-to-insert or insert-to-laminate, was set at 0.2, which was adopted from the literature [14, 39].

Clearances of 1 mm were included in the models. In order to solve convergence problems related to the initial no-contact conditions due to clearances, elastic springs with a stiffness of 1N/mm were introduced between the bolt and a fixed point in the "ground", see Fig. 6. In addition, automatic stabilisation of 1 x 10^{-5} was utilised in the step module to prevent numerical instabilities.

Linear eight-node brick (first-order hexahedral elements) elements with reduced integration, C3D8R, were employed to mesh the composite joints. The contact interaction analyses are very sensitive to the mesh type and the use of quadratic elements is discouraged due to convergence problems. A fine mesh schedule was designed at the bolt hole for accurate and converged numerical predictions, while coarse meshes were utilised far away from the fastener hole to reduce the computational costs. The results of the finite element analyses will be given in the following section, together with the experimental results where necessary.

3. Results and discussion

3.1 Non-pretensioned bolted joints with and without inserts

The load-displacement curves of the bolted joints with and without inserts (three replicas each), with a clearance of 1 mm and finger tightened, are shown in Fig. 7. In the initial stage of the load-displacement curves, slip due to the clearances is observed. In the B2 test, the slip takes place after taking some load, which is attributed to some

unintended clamping force as a result of finger-tightening the bolt. The difference in the amount of slip between the tests is due to the position of the bolt in relation to the hole, which was not controlled during the assembly of the joints.

After slip, the load-deflection response of only-bolted joints (B tests) has a region that appears to be linear up to a load of around 15 kN, followed by unstable non-linear behaviour and a reduction in stiffness, which indicates the unstable development of internal damage. Slight cracking sounds were also heard at a load level of around 15 kN during the tests.

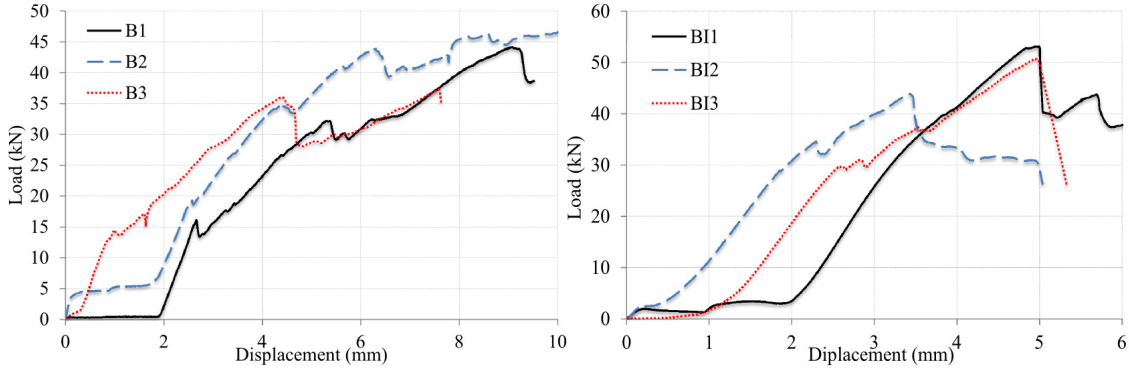

Fig. 7. Load-displacement curves for bolted connections without (B) and with inserts (BI)

The load-displacement behaviour of bolted joints with inserts (BI tests) is almost linear up to a load of 30-35 kN, after which a reduction in stiffness is noted until a sudden load drop. It indicates that, at this load level, bearing damage to the material begins. Small audible cracking sounds were heard at this load level and they were continuous up to the sudden load drops. After initial damage, the joints with inserts manage to accommodate additional load in a stable manner. This is attributed to the insert laps, which act as lateral constraints, preventing the delamination of the FRP laminates and through-thickness expansion around the hole in the insert area. The damage in the laminate is therefore delayed until it splays outside the diameter of the insert lap, where an expansion of the through-thickness of the laminate occurs (see Fig. 8). During the occurrence of the through-thickness expansion, load drops in the load-displacement curves are observed. After the load drop, the joints continue to support lower loads and damage in the laminate expands outside the insert region.

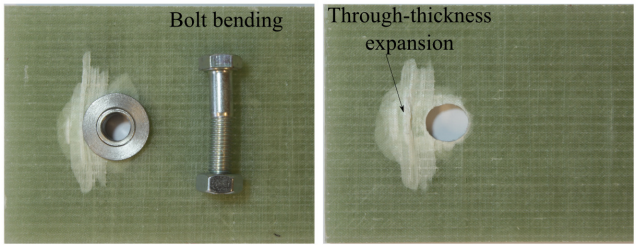

Fig. 8. Failure mode of the bolted joints with inserts (BI tests)

The inserts are efficient in spreading the radial bearing stresses to the laminates and consequently reducing the high stress concentrations occurring in the bearing plane in the laminate. In Fig. 9, the distribution of the bearing stresses in the mid-thickness of

the insert and the laminate is shown for a load of 9.2 kN, resulting from the finite element analyses.

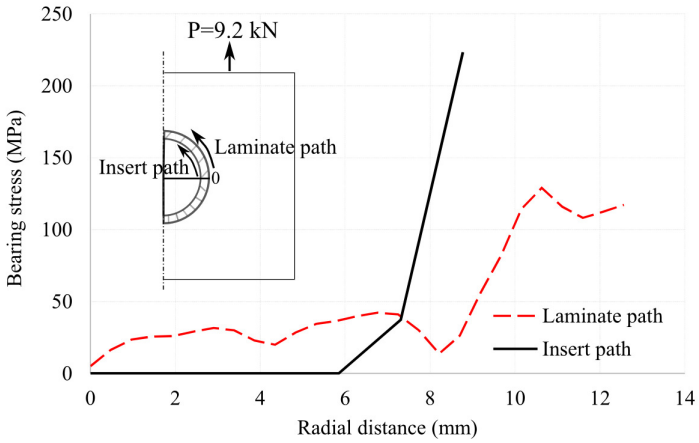

Fig. 9. Radial bearing stresses in the insert and the laminate as a result of FE analyses

The insert also modifies the distibution of the bearing stresses through the thickness, see Fig. 10. Unlike the bearing stresses through the thickness of the insert, the peak bearing stresses through the thickness of the laminate are somewhat in the centre of the laminate. This is due to the lateral constraint effect of the insert laps, which exert compressive stresses on the laminates in the through-thickness direction, thereby modifying the results of the bearing through-thickness stress distributions.

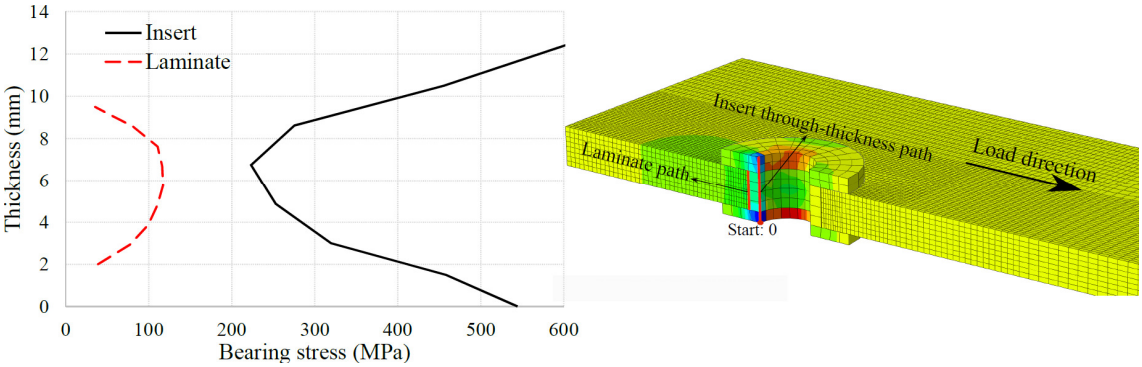

Fig. 10. Finite element bearing stress results through the thickness of the laminate and insert

The initial average stiffness of the only-bolted joints and the bolted joints with inserts was computed from the load-displacement curves as 20.9 kN/mm and 21.3 kN/mm. The stiffness of the joints with inserts is slightly higher, but the difference is negligible.

The failure mode was bearing for all the only-bolted joints. Through-thickness expansion, also referred to as “brooming” failure, at the bolt bearing surface was also observed as depicted in Fig. 11.

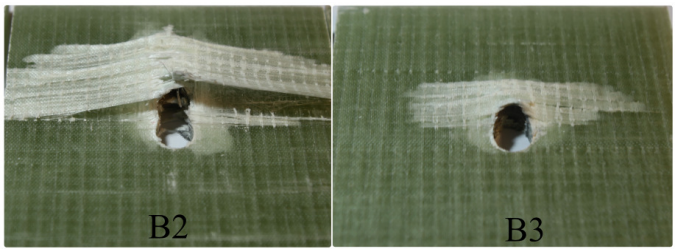

Fig. 11. Failure of only-bolted (B) joints

In the bolted joints with inserts, the typical "brooming" type failure and the through-thickness expansion was prevented by the insert laps. Instead, through-thickness expansion around the outer edge of the insert in the bearing area was observed, as shown in Fig. 8. In addition, yielding of the inserts and the bolts was observed. In bolted joints with inserts, the bolt diameter-to-thickness ratio (d_{bolt}/t) was increased due to a higher thickness bearing to the bolts (thickness of the laminate plus the insert laps), thus permitting bolt bending.

According to the FE analysis, the bolt starts to yield at a load of 26 kN and the insert in the centre laminate at a load of 11 kN, see Fig. 12. The position of the bolt relative to the laminates was modelled in the middle, yielding a slip of 1 mm. It should be borne in mind that the FRP material was modelled as linear elastic and the results might not be totally representative. However, they give an indication of the load levels at which yielding occurs.

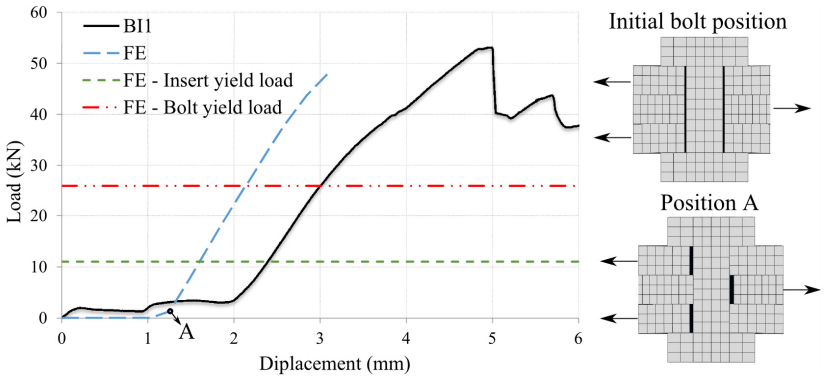

Fig. 12. Comparison of test results with the FE results for bolted joints with insert

3.2 Bolted joints with pretensioned bolts

Five bolted joints with pretensioned bolts were tested. Two of the joints were not loaded to failure in order to prevent yielding and damage to the instrumented bolts. The nominal bolt load was also monitored and is given in the load-displacement curves in Fig. 13, up to the elastic range of the bolt. The displacement represents those measured from LVDT1 in Fig. 3; it thereby includes any extension of the laminate during loading.

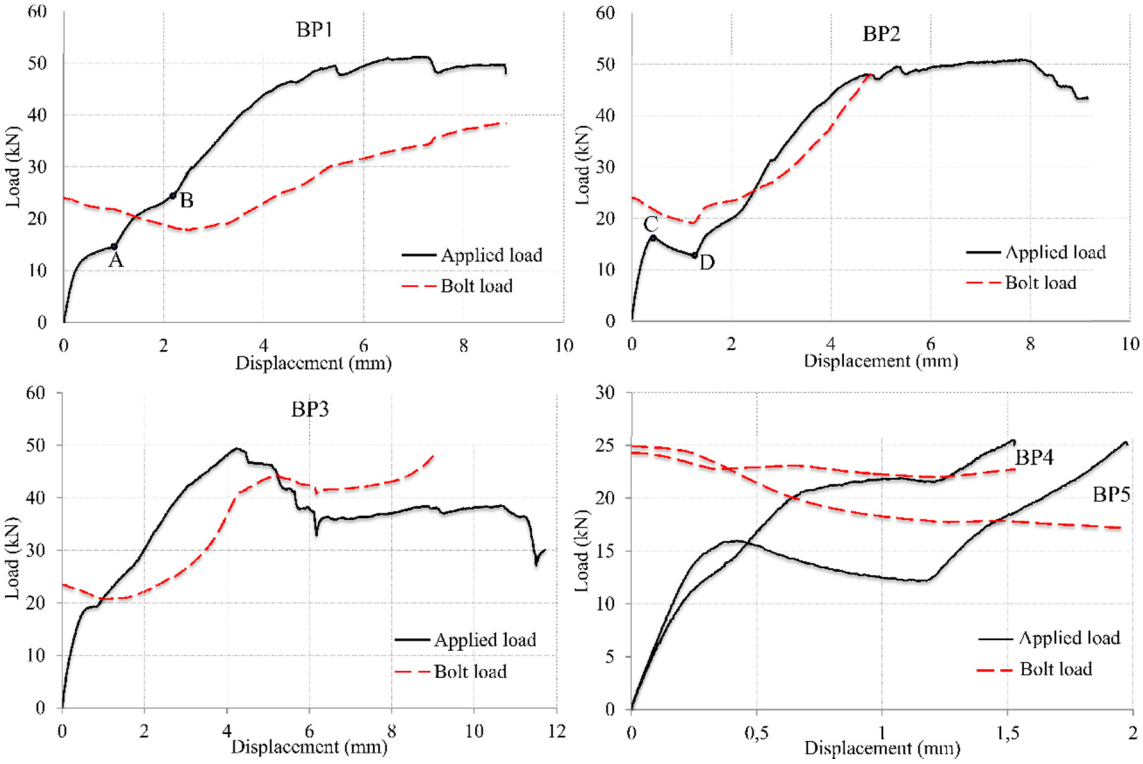

Fig. 13. The applied load and bolt load versus displacement of BP tests

As expected, the joint carries the load through static friction forces (linear initial part of the load-displacement curves) before any slip. At this stage, the joined laminates deform only elastically and no relative displacement between the laminates occurs. Once the applied load exceeds the static friction force, the stage of slip, in which the static friction forces are transformed to kinetic friction forces, begins. The load which causes slip is called the slip load. The slip load is dependent on the bolt preload and the coefficient of friction between the laminates in the following form.

$$F_S = F_P \times \mu_T \times n \qquad (2)$$

where F_S is the slip load, F_P is the bolt preload at the time of slip, μ_T is the friction coefficient of the joint member interfaces and n is the number of friction surfaces, which is two in these tests.

The slip load in these tests is regarded as the peak load before any slip occurs. Based on Equation 2, the coefficient of friction between the laminates is computed and reported in Table 4. The laminates in the BP1 test had a smoother surface than in the other tests and a lower coefficient of friction was justifiable. If the mid-laminate is initially in contact with the bolt, any additional load from bearing is supported by the bolt before any visual slip. This might be the case for the BP3 test, which carries higher loads before any visible slip, yielding, according to the calculations, a higher coefficient of friction compared with the other tests. The coefficient of friction calculated for BP3 might therefore be erroneous.

Table 4. Data and results of the bolted joint tests with preload

Specimen	**BP1**	**BP2**	**BP3**	**BP4**	**BP5**
Initial bolt preload (kN)	24.0	24.1	23.5	24.3	25.0
Clamping pressure (MPa)	82.7	82.9	80.9	83.8	86.0
Slip load: F_s (kN)	12.2	16.3	18.0	13.9	15.9
Bolt preload at slip: F_P (kN)	22.76	22.0	22.3	22.8	22.57
Coefficient of friction	0.27	0.37	0.40	0.31	0.33

During the slip stage, the loads are transferred purely by kinetic friction or a combination of kinetic friction and bearing resistance, depending on the bolt position. For instance, in the BP1 test, the mid-laminate slips before coming into contact with the bolt shank (point A in Fig. 13) and it starts carrying the load in bearing and kinetic friction until the bolt comes in contact with the other two edge laminates (point B in Fig. 13). In the BP2 test, the loads are only transferred via kinetic forces during the slip stage (parts C-D in Fig. 13). Because the kinetic forces are lower than the static ones, a load drop during the slip stage is observed.

After the slip stage is completed, the plates are loaded in bearing and the loads at this stage are carried by bearing and kinetic friction.

In Fig. 13, the change in bolt load versus the displacement is also given. The plots indicate that the bolt load is decreased at least until the bolt comes fully into contact with all the laminates, after which an increase takes place, as observed in the BP1, BP2 and BP3 tests. One contributory factor to the decrease in bolt load is creep in the laminates. Relaxation tests demonstrate that the bolt preload relaxes considerably in the first few hours, see Section 3.4. In Fig. 14, the bolt preload change in the relaxation tests, in which static loading is not present (see Section 3.4), is compared with the bolt preload in the BP1 test. It can be seen that the bolt preload changes significantly when the specimens are loaded statically and the bolt preload loss is more than the preload loss due only to laminate creep.

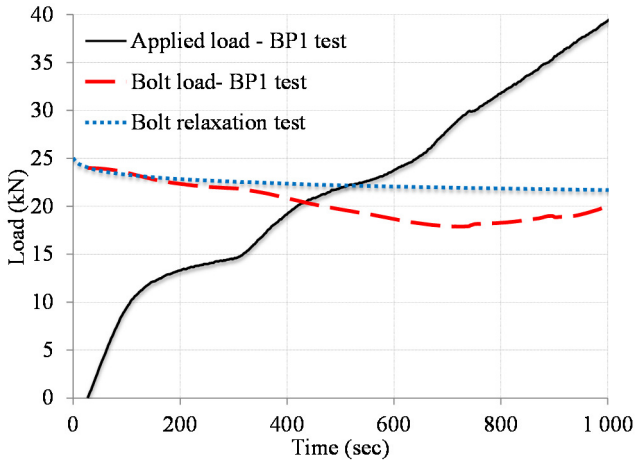

Fig. 14. Comparison of the bolt preload in the relaxation test with the preloaded bolt in the BP1 test

Other contributory factors to the bolt preload reductions include laminate thinning due to in-plane tensile stresses (i.e. from the Poisson effect), which cause a reduction in the elongation of the bolt. The plastification of the bolt in the threaded part of the engaged

shank and bolt thread slip are two other possible effects that cause the relaxation of the initial bolt preload.

Once the bolt comes into full contact with all the laminates, it starts elongating, due to the bending of the bolt shaft, adding to the elongation of the bolt due to the preload; the axial bolt load thus begins to increase. During the onset of damage in the material, which can be seen in Fig. 13, the increase in the bolt load continues. Similar results were also obtained by Tong [9].

The failure mode of all joints was similar. The BP3 test was continued to higher displacements in order to further observe the failure mode shown in Fig. 15. The failure was progressive in nature, spreading out in the entire area of the end distance of the joint. Delaminations and the shear-out of the plies were observed in the through-thickness of the laminate in the end distance. Due to friction, part of the mid-laminate was shoved and attached to the other laminate, referred to as block shear-out in Fig. 15. The failure mainly occurred in the laminate and only slight plastic deformation of the bolt could be seen with the naked eye.

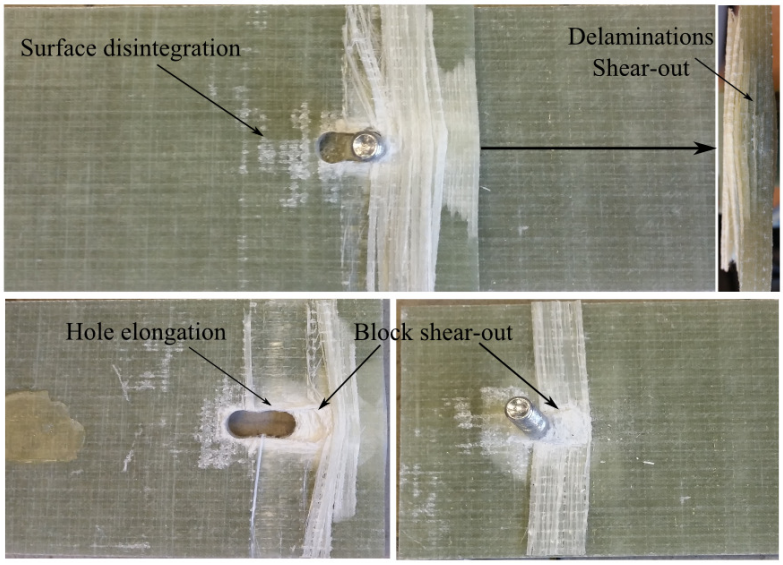

Fig. 15. Failure in the BP3 test

In all the tests, surface disintegration in the form of fibre breakage was observed due to friction. The same type of surface disintegrations was reported by Herrington and Sabbaghian [40] when joints with high clamping forces were tested.

3.3 Bolted joints with inserts and pretensioned bolts

A series of tests was conducted on bolted joints with inserts in which the bolts were pre-tensioned to approximately 24-25 kN. Initially, tests were conducted on joints with inserts as received from the workshop. Subsequently, the inserts were processed through thermal spraying in order to increase the coefficient of friction between the insert surfaces. Layers of tungsten carbide with a thickness of 0.1 ± 0.03 mm were sprayed onto the surfaces of the inserts. The tests with untreated inserts are designated as BIP and the ones with treated inserts as BIPF.

The load-displacement curves of the joints with untreated inserts are given in Fig. 16. The behaviour of these joints is similar to that of the bolted joints with preload. However, the slip load is less than in the BP joints. This is due to the low coefficient of friction between the steel inserts. They were computed to vary between 0.1 and 0.2. In order to verify the coefficient of friction between the inserts, additional tests were conducted with various bolt preloads and the results confirmed that the coefficient of friction between the inserts varied between 0.1 and 0.2.

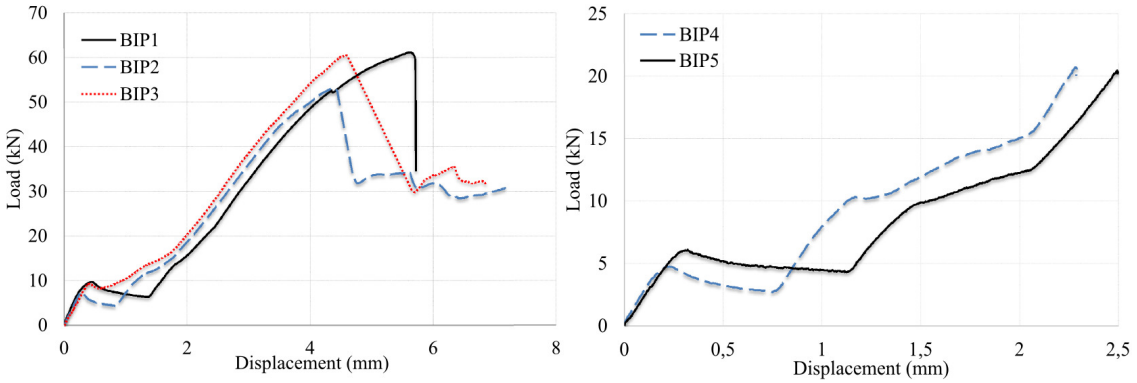

Fig. 16. Load-displacement curves of the bolted joints with untreated inserts with preload

Due to the low coefficient of friction between the inserts, the inserts were modified to increase the coefficient of friction and five tests with the same configuration and instrumentations were carried out, two of which were loaded to final failure.

The results indicate that the loads that can be carried prior to slip are increased, which is related to a much higher coefficient of friction between the insert surfaces, see Fig. 17. The static coefficients of friction for the treated inserts were computed in the same way as that described in Section 3.2 and were found to vary between 0.41 and 0.7. This demonstrated that the thermal spraying method with tungsten carbide was effective when it came to increasing the coefficient of friction.

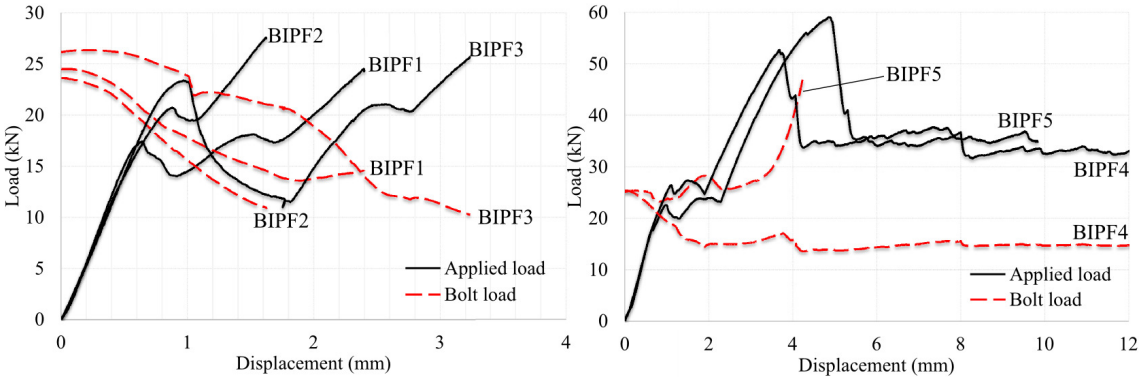

Fig. 17. Load and bolt load versus displacement curves for BIPF tests

The displacement at which slip occurs for the bolted joints with inserts and bolt preload is higher than in the only-bolted joints with preload (BP joints in Fig. 13). This is attributed to the force transfer mechanism for each case. The composite laminates are clamped in the BP tests, whereas, in the BIP tests, the bolt preload is taken by the inserts and barely any clamping force is imposed on the laminate. In the BP tests, when the mid-laminate is initially pulled, the load is resisted by friction forces between the

laminates. In the BIP tests, as soon as the laminate is pulled, it bears instantly on the insert, while the insert resists the load through static friction forces due to the clamping force. Because the laminate bears on the insert, it elongates, yielding higher measured displacements in the LVDT1 transducer. The mechanism of the load transfer for both cases is illustrated in Fig. 18.

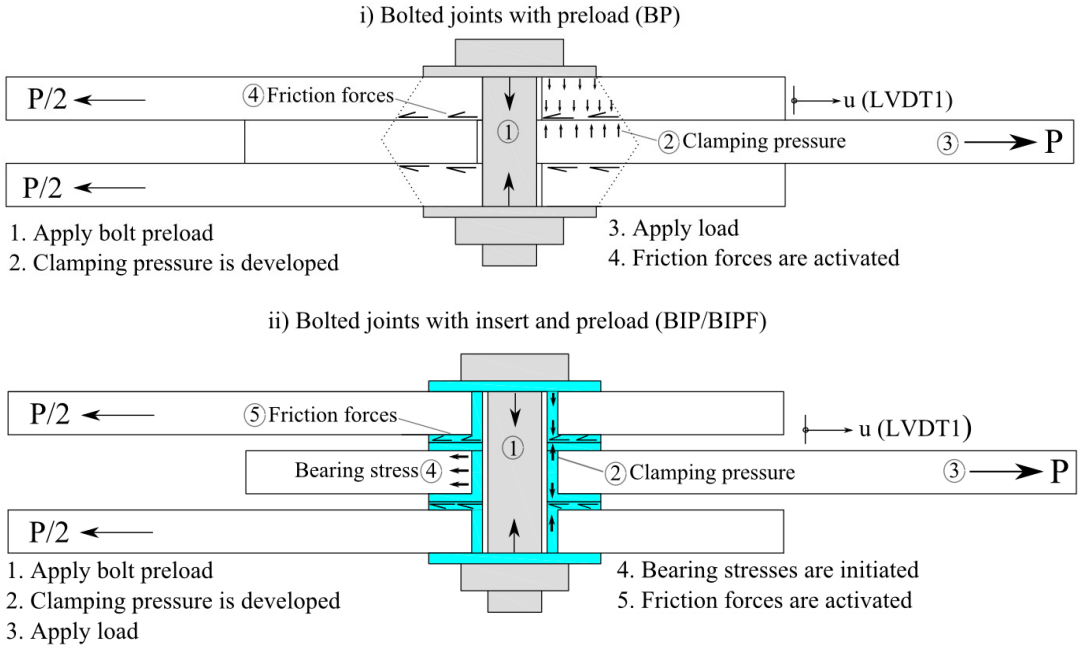

Fig. 18. Mechanism of load transfer before slip for BP and BIP/BIPF joints

The failure mode of the bolted joints with inserts (treated and untreated) with preloaded bolts was similar to those of bolted joints with inserts (BI tests). At the first peak load drop, through-thickness expansion outside the insert outer diameter occurred. In the BIPF4 joint, failure continued to progress in the FRP laminate; the hole elongated, accompanied by delamination and the tearing off of the first plies of the laminates, see Fig. 19. In the BIP5 test, the hole elongation was not as pronounced, but the bolt deformed more than in the BIP4 test. It should also be noted that the BIP4 test was loaded to higher displacements than the BIP5.

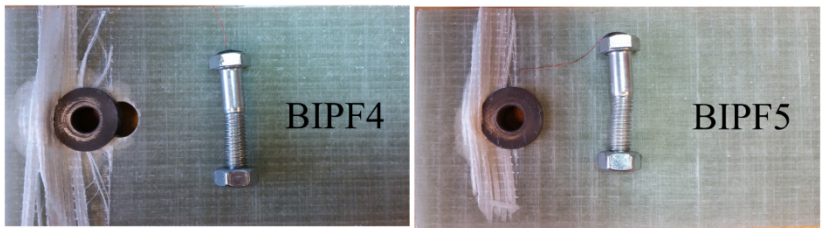

Fig. 19. Failure pattern of BIPF4 and BIPF5 tests

In addition, the inserts in the mid-laminate were plastically deformed. The other tests were not loaded to failure, but slight plastic deformation of the mid-insert occurred.

The finite element analyses showed that for a coefficient of friction of 0.15 between the inserts, the yielding of the insert and bolt starts at a load level of 14 kN and 18 kN respectively. When the inserts have a coefficient of friction of 0.5, yielding begins at a load level of 17 kN and 28 kN respectively, see Fig. 20. The reason for the higher

yielding load in the case of a higher coefficient of friction is attributed to the fact that a larger part of the tensile load is carried by friction and the bending of the bolts and bearing on the inserts is therefore less significant.

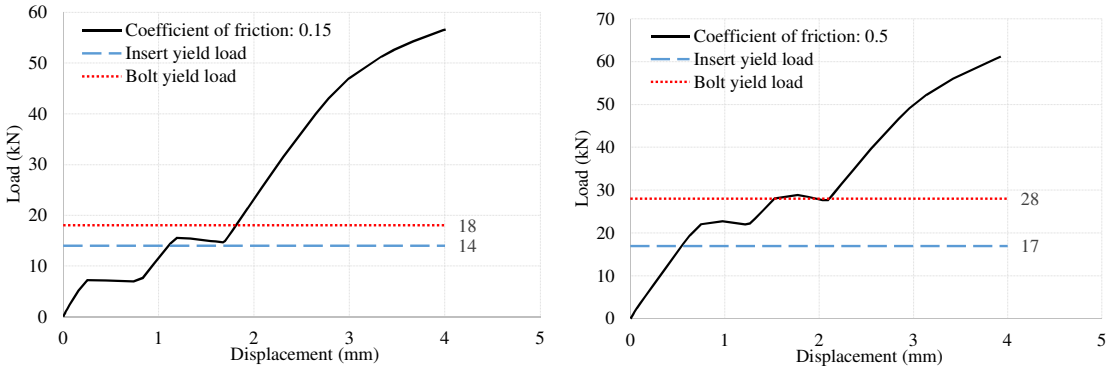

Fig. 20. Finite element results for joints with inserts with a preload with a different coefficient of friction between the insert faces

Before the peak load drop in all the tests, the load-displacement curves show some non-linearity. This is attributed to the accumulation of internal damage under the insert area. During testing, continuous small cracking sounds were audible before the peak load drop. The loads that could be carried in the tests of bolted joints with inserts and preloads are higher than the loads in the tests with inserts without any preload. This additional load is attributed to the additional transfer of forces through kinetic friction. Moreover, the confinement effect of the insert laps (described in Section 3.1) in these tests is even greater, due to the bolt preload. This is the reason that no damage initiation load is as pronounced in these tests as in the BI tests.

3.4 Bolt preload relaxation tests

To analyse the relaxation of the bolt preload in bolted joints with and without inserts, six double-lap, bolted joints were prepared and monitored for approximately 29 days at room temperature in dry conditions. The bolts were tightened at an initial clamping force of 25 kN.

The results for the bolt preload relaxation are given in Fig. 21. RBP1 and RBP2 represent double-lap, only-bolted joints that were re-tightened to 25 kN after 24 hours, RPB3 and RBP4 represent the double-lap, only-bolted joints and RBIP1 and RBIP2 represent the double-lap, bolted joint with inserts. The data logging took place every second during the first hour, every minute during the next 23 hours and every hour during the remainder of the test. Three of the tests (RBIP2, RBP2 and RBP4) were stopped a few days before the final conclusion of the test.

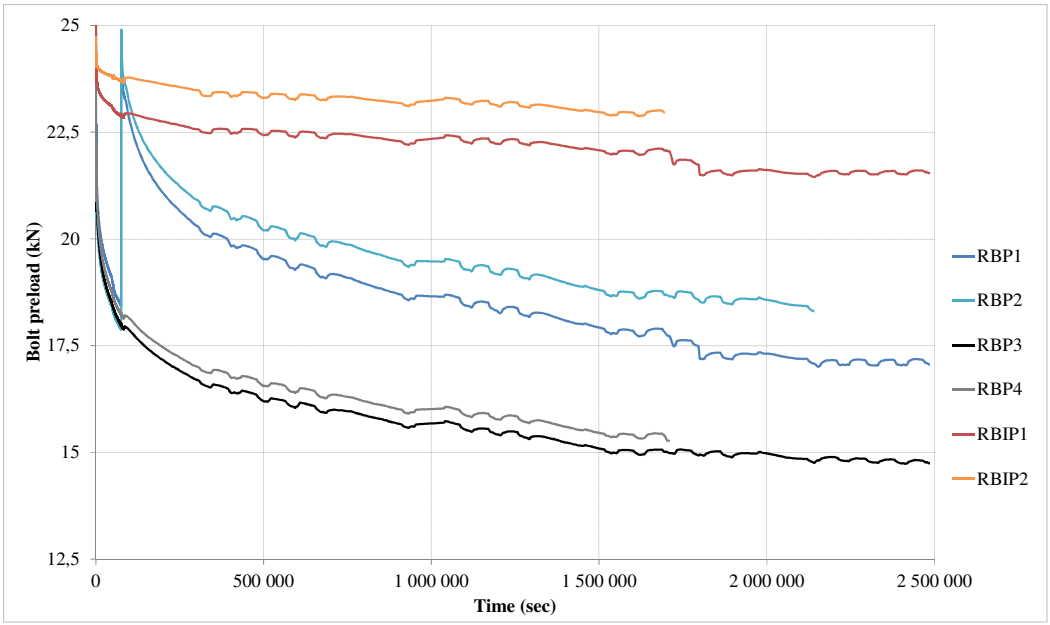

Fig. 21. Bolt load relaxation for composite bolted joints with and without inserts

The fluctuations in the measured bolt load are due to slight temperature fluctuations in the room conditions, which affect the reading on the strain gauge instrumented in the bolt. The results indicate approximately 40% relaxation in the bolt preload for room-temperature-dry conditions after 29 days for only-bolted joints. Even if the bolts are re-tightened to the same clamping force after 24 hours, the relaxation was still significant up to 30%. As expected, the bolt preload relaxation for the joints with inserts is much less and a maximum relaxation of around 15% is recorded. The relaxation is less because the bolt load is mainly accommodated by the steel inserts, while very little to almost nothing is supported by the laminate. According to the FE-analyses, a clamping pressure of a maximum of 9 MPa is exerted on the laminate in the joints with inserts.

The differences between the bolt preload relaxation for the same type of joints could be due to small variations in the amount of the given bolt preload and in the laminate thickness.

The results in Fig. 21 indicate that a considerable amount of the bolt preload loss occurs during the initial hours. After the short term relaxation the first few hours, the long term relaxation continues asymptotically at a nearly constant rate.

It should be noted that these results only relate to the specimens without any external load. External loading can change the bolt preload relaxation and, in reality, external loading will always be present in a structure. As observed in the static tests of the joints with bolt preload, the bolt preload loss is higher during static loading. It is therefore important to take account of the bolt preload loss due to static loading in the design of joints.

4. Concluding remarks

Static tests have been conducted on single-bolted, double-lap composite joints loaded in shear. In addition to a conventional bolted joint configuration, joints with metal inserts were studied. In both cases, the effect of possible bolt pretensioning on the performance

of the joint was studied. In addition, bolt relaxation tests were performed on joints with and without inserts. The conclusions of this study are summarised below.

- The use of metallic inserts in this study offers two main benefits compared with the only-bolted joints. First, the inserts are able to spread and distribute the radial bearing stresses to the laminates. As a result, the high stress concentration occurring in the bearing plane of the laminates is reduced, thereby delaying the damage initiation. These findings are in agreement with those of previous studies in the literature. In addition, the damage in the laminate is delayed by the suppression of the through-thickness expansion in the FRP laminate due to the confining effect of the insert laps, making this the second benefit of the insert. These benefits of the insert make it possible to achieve higher loads before any damage occurs in the laminate compared with the only-bolted joints. These features of the insert also change the through-thickness bearing stress concentrations. In the only-bolted joints, the bearing stresses are concentrated at the edges of the laminate in the hole, whereas, in bolted joints with inserts, the bearing stresses tend to be greatest in the middle of the through-thickness of the laminate. Regarding the stiffness, the effect of the insert is negligible compared with the only-bolted joints.
- The advantages of the bolt preload in terms of stiffness and damage load could be seen in the bolted joints with preload. However, due to high bolt preload relaxation, it is not possible to rely on these benefits. The bolt preload relaxation is fairly significant in the only-bolted joints due to the viscoelastic nature of the composite material. The bolt preload relaxation can be considerably reduced using steel inserts in bolted joints, because the bolt preload goes through the inserts and hardly through the laminates. This makes it possible to rely on the bolt preload benefits, which are ignored in the case of only-bolted joints. However, the bolt preload losses were fairly significant in the statically loaded joints. This should be taken into account in the design of joints if the bolt preload is accounted for.
- Depending on the coefficient of friction between the inserts, the load carried by the joint before any slip can be increased considerably in the serviceability limit state. In addition, the stiffness of the bolted joints with inserts and preloads is considerably higher compared with the joints without any bolt preload.
- Bolted joints with inserts and preloads were the most efficient in terms of initial damage load and the ultimate maximum load. These joints are promising when it comes to providing slip-resistant joints in the service state of FRP bridges. However, additional tests are required for these joints to further validate the conclusions that are drawn.

The number of tests performed in this paper was not extensive enough to evaluate the data statistically, but they gave strong indications of the static behaviour of the different kinds of joint. All the tests were performed in laboratory conditions and any effect of temperature or moisture was not taken into account. It is suggested that future work should focus on studying the behaviour of the proposed joints in different service conditions.

Acknowledgements

The authors would like to acknowledge the support provided by FiberCore Europe, the manufacturer of the material in the test specimens.

References

1. Handbook-MIL-HDBK M. 17-3F: Composite Materials Handbook, Volume 3-Polymer Matrix Composites Materials Usage, Design, and Analysis. 2002, US Department of Defense.
2. Girão Coelho AM and Mottram JT. A review of the behaviour and analysis of bolted connections and joints in pultruded fibre reinforced polymers. Materials & Design, 2015. **74**(0): p. 86-107.
3. Turvey GJ. 3 - Bolted joints in pultruded glass fibre reinforced polymer (GFRP) composites, in Composite Joints and Connections, P. Camanho and L. Tong, Editors. 2011, Woodhead Publishing. p. 77-111.
4. Ascione F, Feo L and Maceri F. An experimental investigation on the bearing failure load of glass fibre/epoxy laminates. Composites Part B: Engineering, 2009. **40**(3): p. 197-205.
5. Zafari B and Mottram JT. Effect of orientation on pin-bearing strength for bolted connections in pultruded joints. In 6th International Conference on FRP Composites in Civil Engineering 2012. Rome, Italy.
6. Turvey GJ. Single-bolt tension joint tests on pultruded GRP plate — effects of tension direction relative to pultrusion direction. Composite Structures, 1998. **42**(4): p. 341-351.
7. Ireman T, Ranvik T and Eriksson I. On damage development in mechanically fastened composite laminates. Composite Structures, 2000. **49**(2): p. 151-171.
8. Erki MA. Bolted glass-fibre-reinforced plastic joints. Canadian journal of civil engineering, 1995. **22**(4): p. 736-744.
9. Tong L. Bearing failure of composite bolted joints with non-uniform bolt-to-washer clearance. Composites Part A: Applied Science and Manufacturing, 2000. **31**(6): p. 609-615.
10. Turvey GJ and Wang P. Failure of pultruded GRP bolted joints: a Taguchi analysis. Proceedings of the ICE - Engineering and Computational Mechanics, 2009. **162**, 155-166.
11. Lawlor VP, McCarthy MA and Stanley WF. An experimental study of bolt–hole clearance effects in double-lap, multi-bolt composite joints. Composite Structures, 2005. **71**(2): p. 176-190.
12. Schön J. Coefficient of friction and wear of a carbon fiber epoxy matrix composite. Wear, 2004. **257**(3–4): p. 395-407.

13. Mottram JT. Friction and load transfer in bolted joints of pultruded fibre reinforced polymer section, in FRP Composites in Civil Engineering - CICE 2004. 2004, Taylor & Francis. p. 845-850.

14. Olmedo Á and Santiuste C. On the prediction of bolted single-lap composite joints. Composite Structures, 2012. **94**(6): p. 2110-2117.

15. Mottram JT and Zafari B. Pin-bearing strengths for bolted connections in fibre-reinforced polymer structures. Proceedings of the ICE - Structures and Buildings, 2011. **164**: p. 291-305.

16. Ascione F, Feo L and Maceri F. On the pin-bearing failure load of GFRP bolted laminates: An experimental analysis on the influence of bolt diameter. Composites Part B: Engineering, 2010. **41**(6): p. 482-490.

17. Rosner CN and Rizkalla SH. Bolted connections for fiber-reinforced composite structural members: Experimental program. Journal of Materials in Civil Engineering, 1995. **7**(4): p. 223-231.

18. Mara V and Haghani R. Review of FRP decks: structural and in-service performance. 2015. 1-22 DOI: 10.1680/bren.14.00009.

19. Hart-Smith LJ. Design and Analysis of Bolted and Riveted Joints in Fibrous Composite Structures, in Recent Advances in Structural Joints and Repairs for Composite Materials, L. Tong and C. Soutis, Editors. 2003, Springer Netherlands. p. 211-254.

20. Thoppul SD, Gibson RF and Ibrahim RA. Phenomenological modeling and numerical simulation of relaxation in bolted composite joints. Journal of Composite Materials, 2008. **42**(17): p. 1709-1729.

21. Qureshi J and Mottram JT. Resin injected bolted connections: a step towards achieving slip-resistant joints in FRP bridge engineering. In 1st FRP Bridges Conference 2012. London, UK.

22. Clarke JL. Structural Design of Polymer Composites: Eurocomp Design Code and Background Document. 2003, London, UK: Taylor & Francis.

23. Nilsson S. Increasing strength of graphite/epoxy bolted joints by introducing an adhesively bonded metallic insert. Journal of composite materials, 1989. **23**(7): p. 642-650.

24. Camanho PP and Matthews FL. Bonded metallic inserts for bolted joints in composite laminates. Proceedings of the Institution of Mechanical Engineers Part L: Journal of Materials: Design and Applications, 2000. **214**(1): p. 33-40.

25. Kradinov V, Madenci E and Ambur DR. Bolted lap joints of laminates with varying thickness and metallic inserts. Composite Structures, 2005. **68**(1): p. 75-85.

26. Camanho PP, Tavares CML, de Oliveira R, et al. Increasing the efficiency of composite single-shear lap joints using bonded inserts. Composites Part B: Engineering, 2005. **36**(5): p. 372-383.

27. Herrera-Franco PJ and Cloud GL. Strain-relief inserts for composite fasteners. An experimental study. Journal of Composite Materials, 1992. **26**(5): p. 751-768.

28. Rispler AR, Steven GP and Tong L. Photoelastic evaluation of metallic inserts of optimised shape. Composites Science and Technology, 2000. **60**(1): p. 95-106.

29. Mirabella L and Galea SC. An experimental investigation into the use of inserts to enhance the static performance of thin composite bolted lap joints. In Eleventh International Conference on Composite Materials. 1997. Queensland, Australia: Australian Composite Structures Society Woodhead Publishing Limited.

30. ASTM. Standard D3039/D3039M−14: Standard Test Method for Tensile Properties of Polymer Matrix Composite Materials. 2014, ASTM International: United States.

31. ASTM. Standard D3410/D3039M−03: Standard Test Method for Compressive Properties of Polymer Matrix Composite Materials with Unsupported Gage Section by Shear Loading. 2014, ASTM International: United States.

32. ASTM. Standard D7078/D7078M−12: Standard Test Method for Shear Properties of Composite Materials by V-Notched Rail shear method. 2014, ASTM International: United States.

33. Highsmith AL and Reifsnider KL. Stiffness-reduction mechanisms in composite laminates. Damage in composite materials, ASTM STP, 1982. **775**: p. 103-117.

34. Reifsnider KL and Masters JE. Investigation of characteristic damage states in composite laminates. American Society of Mechanical Engineers (Paper), 1978(78 WA/Aero-4).

35. ASTM. Standard D5961/D5961M−13: Standard Test Method for Bearing Response of Polymer Matrix Composite Laminates. 2013, ASTM International: United States.

36. Zhao Y. Torque limit for bolted joint for composites, in Part A: TTTC properties of laminated composites. 2002, Nasa faculty fellowship program: Alabama, USA.

37. Thomas FP and Zhao Y. Torque limit for composites joined with mechanical fasteners. In Structural Dynamics and Materials Conference. 2005. Austin, TX; United States.

38. EN-1003-1-8. Eurocode 3: Design of steel structures - Part 1-8: Design of joints. 2005, European Committee for Standardisation: Brussels.

39. Egan B, McCarthy MA, Frizzell RM, et al. Modelling bearing failure in countersunk composite joints under quasi-static loading using 3D explicit finite element analysis. Composite Structures, 2014. **108**(0): p. 963-977.

40. Herrington PD and Sabbaghian M. Factors affecting the friction coefficients between metallic washers and composite surfaces. Composites, 1991. **22**(6): p. 418-424.